

Butanolysis of 4-methylbenzenediazonium ions in binary n-BuOH/H₂O mixtures and in n-BuOH/SDS/H₂O reverse micelles. Effects of solvent composition, acidity and temperature on the switch between heterolytic and homolytic dediazonation mechanisms

Alejandra Fernández-Alonso, M^a José Pastoriza Gallego and Carlos Bravo-Díaz*

Received 19th May 2010, Accepted 22nd July 2010

DOI: 10.1039/c0ob00143k

We investigated the effects of solvent composition, acidity and temperature on the switch between heterolytic and homolytic mechanisms in the course of the butanolysis of 4-methylbenzenediazonium (4MBD) ions in binary BuOH/H₂O mixtures and in reverse micelles, RMs, composed of n-BuOH, H₂O and sodium dodecyl sulfate, SDS, by employing a combination of spectrometric (UV/vis) and chromatographic (HPLC) techniques. In reaction mixtures with high n-BuOH percentages, S-shaped variations of k_{obs} with acidity, defined hereafter as $-\log[\text{HCl}]$, are obtained with rate enhancements of up to ~370-fold on going from $-\log[\text{HCl}] = 2$ to 6, with inflection points at $-\log[\text{HCl}] \sim 4$. HPLC analyses of the reaction mixtures show that the substitution product 4-cresol, ArOH and the reduction product toluene, ArH, are formed competitively. The variation of their yields with acidity is also S-shaped, so that at high acidities ($-\log[\text{HCl}] < 3$) only traces of ArH are detected but on lowering the acidity, the reduction product ArH becomes predominant. The largest variations of k_{obs} and of the product yields with acidity are found in the $-\log[\text{HCl}] = 3\text{--}5$ range, suggesting that a turnover in the dediazonation mechanism takes place under acidic conditions. The results can be interpreted in terms of two competitive reaction pathways, one heterolytic, involving a rate-determining formation of an extremely reactive aryl cation that traps the nucleophiles available in its solvation shell leading to the formation of substitution products ($\text{D}_{\text{N}} + \text{A}_{\text{N}}$ mechanism) and a second route where the BuOH reacts with 4MBD to yield an unstable O-adduct of the type Ar-N=N-O-R (diazo ether) in a rapid pre-equilibrium step that initiates a radical process leading to the formation of the reduction product ArH (O-coupling mechanism). The results illustrate how the heterolytic and homolytic mechanisms can be switched by just changing the acidity of the solution. Kinetic analyses of the variations of k_{obs} with acidity at different temperatures allowed us to separate k_{obs} into the components for the heterolytic pathway, k_{HET} , and that for the homolytic one, k_{HOM} , to determine relevant thermodynamic parameters for both reaction pathways and for the equilibrium constant K for the formation of the O-adduct Ar-N=N-O-R .

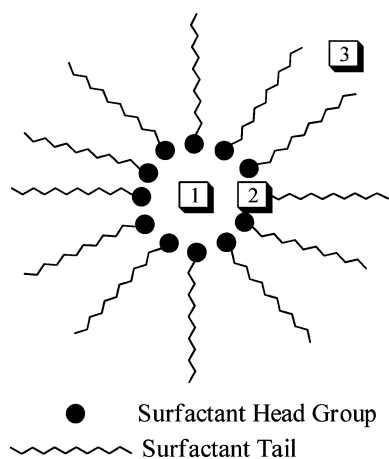
Introduction

Solvolytic studies in mixed solvents have an advantage of providing the opportunity to vary continuously the reaction conditions compared to the more abrupt changes usually found when changing the nature or position of substituents. However, solubility problems may arise preventing systematic studies on individual substrates over the whole composition range. This is the case of binary water–alcohol mixtures, where the short chain alkyl alcohols ($\text{C}_n\text{H}_{2n+1}\text{OH}$, $n < 3$) such as MeOH or EtOH, are miscible with water at any proportion but alcohols with longer alkyl chains ($n \geq 4$) have limited solubility in water. For instance, n-BuOH is partially soluble in water and only binary systems containing percentages of n-BuOH ranging 0–10% and ~90–100% can be prepared, but pentanol is essentially insoluble at any proportion.

To overcome the solubility problem, we propose the use of reverse micelles as reaction media. Reverse micelles (RMs), Scheme 1, are thermodynamically stable aggregates in which nanoscale droplets of a polar liquid, usually water, are surrounded by a surfactant layer and distributed uniformly in a nonpolar continuous phase. The centre of the RMs, the so-called water pool, Scheme 1, provides a unique reaction site because of the “tailored” sizes that can be achieved with these systems.^{1–4} The water in the water pool may have different properties depending on the ratio $w_0 = [\text{H}_2\text{O}]/[\text{SURF}]$, and can be used in place of polar organic solvents to carry out chemical reactions.^{5–7} Hence, the systems of the “surfactant–water–organic solvent” type, Scheme 1, find useful application in preparative chemistry including chemical transformations of water-insoluble substances, preparation of nano-size particles and in bioorganic synthesis.^{5,8–10} RMs can also be considered as a model of biomembrane fragments and can be seen as an approach to better understanding the role of biomembrane environments in biocatalysis.^{11–14}

The use of RMs as reaction media may have significant effects on the chemical reactivity because such organized systems introduce

Universidad de Vigo, Facultad de Química Dpt., Química Física, 36200 Vigo, Spain. E-mail: cbravo@uvigo.es; Fax: 34 986 812556; Tel: 34 986 812303



Scheme 1 Basic representation of a reverse micelle showing the different regions of the micellar solution: 1) water pool, 2) interface, 3) organic phase—in the present work, *n*-BuOH.

new environments that may have large effects on the physical properties of the substrate^{11,15–18} such as stabilization of ground or excited states, acid–base and redox equilibria, and so forth. RMs may also be very interesting for solvolytic studies and a number of solvolytic reactions have been exploited to gain insights into the properties of the RMs and those of the encapsulated water.^{14,19–22} In addition, RMs allow preparation of reaction mixtures containing a wide range of percentages of alcohol ($n \geq 4$) in the system,^{11,23,24} and for instance, reverse micelles containing percentages of BuOH in the range 40–90% can be easily prepared by adding different amounts of sodium dodecyl sulfate, SDS.

Here we take advantage of the distinctive characteristics of organized surfactant molecular assemblies and their unique solubilization characteristics^{1,14,25–28} to expand our previous solvolytic dediazonium studies and, particularly, to further investigate the switch between heterolytic and homolytic dediazoniations, which can be achieved by just changing the acidity of the reaction mixture.^{29–34} Solvolytic dediazoniations in BuOH–H₂O mixtures have not been studied over a wide composition range so far,³⁵ probably because of the mentioned solubility problems, and so the use of reverse micelles allows one to overcome the solubility problem by introducing a new reaction media and, at the same time, the results can be compared with those in binary BuOH/H₂O mixtures to highlight the role of organized systems in the target reaction. For this purpose, a combination of spectroscopic (UV–VIS) and chromatographic (high performance liquid chromatography, HPLC) techniques were used.

The reverse micelles were prepared by using $w_0 = [\text{H}_2\text{O}]/[\text{SURF}] = 42.7$, which allows changes in the percentage of BuOH in the system in the range 45–90% BuOH, a range that cannot be otherwise attained. The ratio $w_0 = 42.7$ was chosen because the size, the shape, and some other relevant structural characteristics of the reverse micellar aggregates formed are known^{36,37} and because the properties of the water inside the water pool are the same as those of bulk water.^{14,19,28} 4MBD was chosen as substrate because substantial knowledge on its spontaneous dediazonium in a number of alcohol–water mixtures^{38–41} and in normal SDS micellar systems is available.⁴² Previous investigations have shown that 4MBD is largely associated with normal SDS micelles ($K_s = 1390 \text{ M}^{-1}$)⁴² and that its dediazonium mechanism is the

Table 1 Effect of the percentage of BuOH on the observed rate constants, k_{obs} , for solvolyses of 4MBD in binary BuOH/H₂O mixtures. [4MBD] = $1.2 \times 10^{-4} \text{ M}$, $T = 50^\circ \text{C}$, $-\log[\text{HCl}] = 2$

% BuOH	$10^4 k_{\text{obs}}/\text{s}^{-1}$
0	2.27 ± 0.01
3	2.46 ± 0.01
6	2.58 ± 0.01
90	7.87 ± 0.03
93	7.51 ± 0.02
96	6.99 ± 0.02
98	7.71 ± 0.02

same as that in pure water.⁴² Moreover, investigations on the dediazonium of structurally similar arenediazonium ions in BuOH/SDS/H₂O reverse micelles showed that they are mostly located in the interfacial region of the reverse micelles,^{41,43} and consequently 4MBD dediazonium is expected to take place primarily in the interfacial region of the RMs, Scheme 1, where a mixture of water, SDS and BuOH is present.

Results

1 Solvolyses of 4MBD in binary BuOH/H₂O mixtures

1.1 Effects of solvent composition on the observed rate constants, k_{obs} , and on the product distribution. Observed rate constants, k_{obs} , were determined spectrophotometrically by monitoring the disappearance of 4MBD as indicated in the experimental section, Table 1. k_{obs} values increase steadily upon increasing the BuOH content in the reaction mixture and an increase of ~4-fold is obtained at 98% BuOH. This modest increase in k_{obs} on increasing [BuOH] is in keeping with that found in previous solvolytic dediazoniations,^{38,39,44,45} and suggests that nucleophilic attack by solvent is not involved in the rate-limiting step of the reaction, consistent with the well known insensitivity of dediazoniations to solvent changes.^{35,39,44,45} The k_{obs} value in the absence of BuOH, $k_{\text{obs}} = 2.27 \times 10^{-4} \text{ s}^{-1}$ is in keeping with that reported in the literature³⁹ for the spontaneous dediazonium of 4MBD at $T = 60^\circ \text{C}$, bearing in mind its activation energy, $E_a = 112 \text{ kJ mol}^{-1}$.

HPLC analyses of the reaction mixtures indicate that at low percentages of BuOH, the major dediazonium product is ArOH (>95%), but its yield goes down to ~30% at 96% BuOH with a concomitant increase in the yield of ArOBu (observed as an increase in the corresponding peak area). Only small amounts (<10%) of the reduction product ArH were detected.

Although ArH is a minor product under our experimental conditions, its formation was previously detected in solvolytic dediazoniations carried out under acidic conditions in the absence of reductants, and its formation was explained in terms of a competitive reaction pathway leading to the formation of highly unstable diazo ethers of the type $\text{ArN}=\text{N}-\text{OR}$, which initiates a radical process.^{40,46} The finding of small amounts of the reduction products ArH in the course of the butanolyses of 4MBD can, therefore, be envisaged as evidence of the potential existence of a competing mechanism, and this possibility was further investigated.

1.2 Effects of acidity and temperature on the observed rate constants, k_{obs} , and on the product distribution. The effects of acidity on k_{obs} were investigated by employing two representative

Table 2 Effects of acidity on k_{obs} values for the decomposition of 4MBD in a 3% binary BuOH/H₂O mixture. [4MBD] = 1.2×10^{-4} M, $T = 50^\circ\text{C}$

$-\log[\text{HCl}]$	$10^4 k_{\text{obs}}/\text{s}^{-1}$
6.00	2.45 ± 0.01
5.00	2.56 ± 0.01
4.00	2.64 ± 0.01
3.00	2.73 ± 0.01
2.00	2.75 ± 0.01
1.00	2.79 ± 0.01
0.50	2.84 ± 0.01
0.25	2.8 ± 0.01

reaction mixtures (3% and 90% BuOH). When employing the 3% BuOH reaction mixture, a change in acidity ($-\log[\text{HCl}] = 0.25\text{--}6$) does not change k_{obs} significantly, Table 2; however, when using the 90% BuOH mixture, parallel changes in acidity lead to S-shaped variations in k_{obs} , as illustrated in Fig. 1. Note that the largest variations in k_{obs} are obtained in the $-\log[\text{HCl}] = 3\text{--}5$ range, compared with those in the $-\log[\text{HCl}] = 1\text{--}3$ and in the $-\log[\text{HCl}] = 5\text{--}6$ range.

The effects of temperature on k_{obs} were also investigated and similar sigmoidal profiles were obtained at all temperatures investigated as shown in Fig. 1. At a given temperature, k_{obs} values increase ~ 10 -fold on lowering the acidity from $-\log[\text{HCl}] = 2$ to $-\log[\text{HCl}] = 6$, and the extent of this increase seems to be independent of temperature. At a given acidity $-\log[\text{HCl}] > 4$, k_{obs} increases ~ 4 -fold on increasing the temperature from $T = 45^\circ\text{C}$ up to $T = 60^\circ\text{C}$, however, the inflection point of the sigmoidal plots seems to be very similar at any temperature.

We also analyzed the effects of acidity on the product distribution at two selected temperatures, and similar S-shaped variations were found, Fig. 2. At high acidity, only small amounts of ArH are obtained, and the heterolytic products are the major dediazonation products; however, on lowering the acidity, a significant increase in the yield of the reduction product ArH is detected with a concomitant decrease in the yields of the heterolytic ones is obtained. A change in the temperature does not seem to have a major effect on the product distribution nor on the inflection points of the sigmoidal profiles, Fig. 2, as was found for the variations of k_{obs} with acidity, Fig. 1.

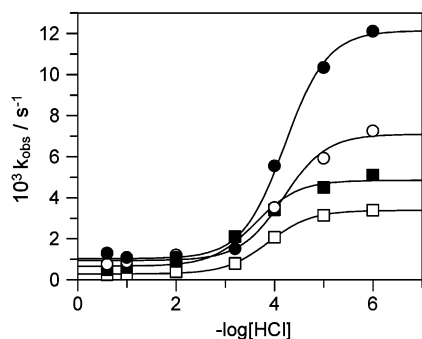


Fig. 1 Effects of acidity and temperature on k_{obs} for the decomposition of 4MBD in a 90% BuOH/H₂O binary mixture. [4MBD] = 1.2×10^{-4} M, $\square T = 45^\circ\text{C}$, $\blacksquare T = 50^\circ\text{C}$, $\circ T = 55^\circ\text{C}$, $\bullet T = 60^\circ\text{C}$.

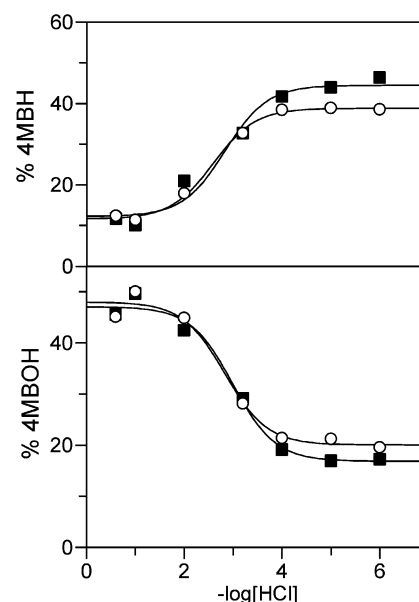


Fig. 2 Illustrative plots of the variation in the yields of the heterolytic ArOH and reduction ArH dediazonation products with acidity and temperature for the decomposition of 4MBD in a binary 90:10 (v/v) BuOH/H₂O mixture. [4MBD] = 1×10^{-3} M, $\blacksquare 50^\circ\text{C}$, $\circ 60^\circ\text{C}$.

2 Solvolyses of 4MBD in reverse BuOH/SDS/H₂O micelles.

2.1 Effects of solvent composition, acidity and temperature on the observed rate constants, k_{obs} , and on the product distribution.

The composition and some structural parameters of the reverse micelles employed are indicated in Table 5. Fig. 3 illustrates the variation of k_{obs} with %BuOH at two selected acidities. At high acidities ($-\log[\text{HCl}] = 1.7$), k_{obs} increases modestly upon increasing the BuOH content of the system. At lower acidities ($-\log[\text{HCl}] = 4.3$), the obtained k_{obs} values at a given %BuOH are much higher than those at high acidity and the increase in k_{obs} on increasing the %BuOH is of ~ 6 -fold, highlighting the enormous effect of acidity on the reaction. These observations prompted us to further investigate the effects of acidity on k_{obs} and on the product distribution.

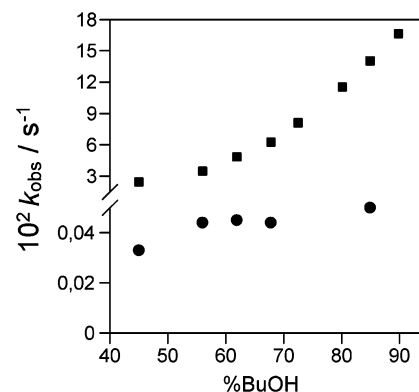


Fig. 3 Effects of the percentage of BuOH in BuOH/SDS/H₂O reverse micelles on k_{obs} for the decomposition of 4MBD. $\bullet -\log[\text{HCl}] = 1.7$, $\blacksquare -\log[\text{HCl}] = 4.3$.

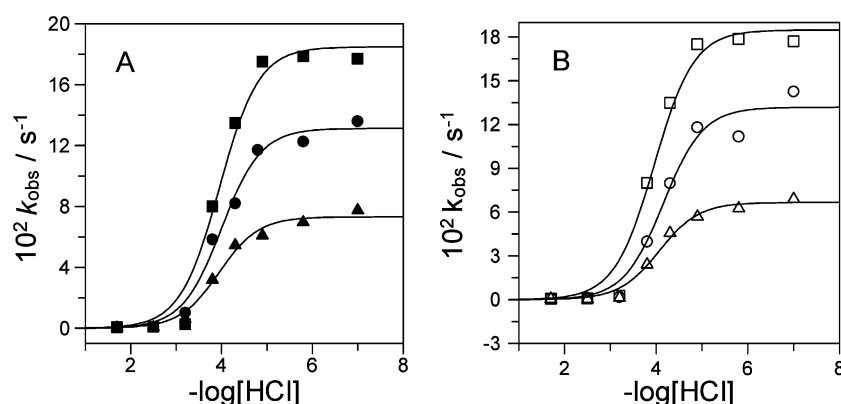


Fig. 4 Effects of acidity on k_{obs} for the decomposition of 4MBD in reverse micelles at selected temperatures. A) $T = 50\text{ }^{\circ}\text{C}$, \blacktriangle 45% BuOH (RM1), \bullet 61.9% BuOH (RM3), \blacksquare 72.5% BuOH (RM5). B) % BuOH = 72.5, \triangle $T = 40\text{ }^{\circ}\text{C}$, \circ $T = 45\text{ }^{\circ}\text{C}$, \square $T = 50\text{ }^{\circ}\text{C}$. [4MBD] $\sim 1 \times 10^{-4}$ M.

Fig. 4 illustrates the effects of acidity on k_{obs} for the solvolyses of 4MBD in selected reverse micelles at constant temperature (Fig. 4A) and in a selected reverse micelle at different temperatures (Fig. 4B). In both cases, S-shaped variations are obtained. At high acidities, $k_{\text{obs}} = 5.5 \times 10^{-4}\text{ s}^{-1}$ (RM5, %BuOH = 72.5, $T = 50\text{ }^{\circ}\text{C}$) and increases ~ 370 -fold on lowering the acidity down to $-\log[\text{HCl}] = 6$. When using RM1 (%BuOH = 45%) and RM3 (%BuOH = 62%), the change in k_{obs} on lowering the acidity is ~ 175 - and ~ 243 -fold, respectively. Similar increases in k_{obs} are obtained on changing the temperature from $T = 40\text{ }^{\circ}\text{C}$ up to $50\text{ }^{\circ}\text{C}$, Fig. 4B, at a fixed %BuOH (RM5). Higher temperatures were not investigated because rate constants become too high to be measured and to minimize potential changes in the structure of the reverse micelles due to the increase in the thermal energy. We are aware that a change in the temperature may lead to some change in the structural parameters of the reverse micelle. We did not investigate this point and thus we cannot quantify the extent of this potential change; however, if any change occurs, it must not be kinetically significant because products are formed competitively, and because the inflection points of the sigmoidal curves are the same at any temperature, both in the binary mixtures and in reverse micelles as we will show in Table 3.

We also analyzed the effects of the percentage of BuOH in the RMs on the product distribution at two selected acidities,

Table 3 Values of k_{HET} , k_{HOM} and of the equilibrium constant K (average values from kinetic and HPLC data), obtained by fitting the experimental data to eqn 1, which can be derived from Scheme 3

$T/^{\circ}\text{C}$	% BuOH	pK	$10^4 k_{\text{HET}}/\text{s}^{-1}$	$10^4 k_{\text{HOM}}/\text{s}^{-1}$
Binary mixture				
45	90	4.9 ± 0.1	2.8 ± 0.3	34 ± 1
50	90	4.6 ± 0.1	7.0 ± 2.0	48 ± 2
55	90	5.2 ± 0.1	9.0 ± 2.0	71 ± 3
60	90	4.9 ± 0.1	15.0 ± 2.0	121 ± 3
Reverse micelles				
40	72.5	5.0 ± 0.1	4 ± 1	670 ± 30
50	72.5	4.8 ± 0.1	5.5 ± 0.8	1830 ± 40
45	72.5	5.0 ± 0.1	5.0 ± 1	1320 ± 70
50	45	4.6 ± 0.1	4.0 ± 0.8	730 ± 80
50	62	4.9 ± 0.1	5.6 ± 0.4	1310 ± 50

Fig. 5. At high acidity ($-\log[\text{HCl}] = 2.5$) and low BuOH content, the major dediazonation product is ArOH. Upon increasing the BuOH content, the yield of the reduction product ArH remains practically constant. Note that at 90% BuOH, Fig. 5A, the yield of ArH is the same as that obtained in binary mixtures at the same acidity, Fig. 2. This contrasts with the variation in the yield of ArOH, which decreases upon increasing [BuOH] because of the competitive formation of the substitution product ArOBu.

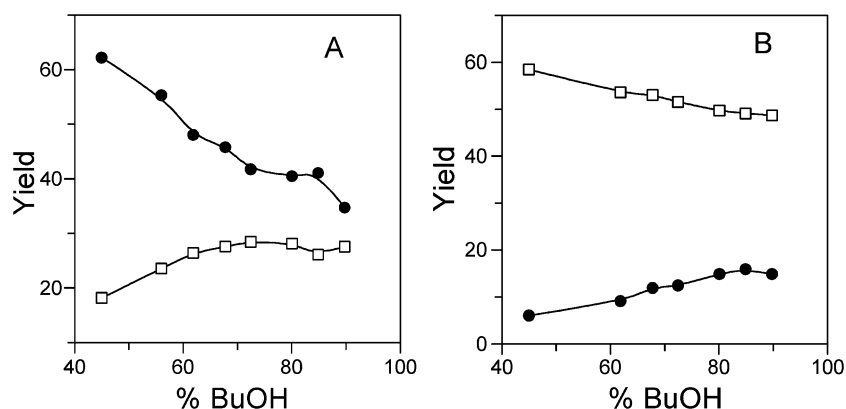


Fig. 5 Effect of the %BuOH on product distribution for the decomposition of 4MBD in reverse micelle BuOH/SDS/ H_2O . $\log[\text{HCl}] = 2.5$ (left) and $-\log[\text{HCl}] = 4.3$ (right). Solid lines drawn to aid the eye. \square 4MBH and \bullet 4MBOH. [4MBD] $\sim 1 \times 10^{-3}$ M, $T = 50\text{ }^{\circ}\text{C}$.

On lowering the acidity ($-\log[\text{HCl}] = 4.3$), Fig. 5B, the major dediazonation product becomes ArH , suggesting that a change in the dediazonation mechanism has taken place, and its yield seems to decrease slightly upon increasing the BuOH content.

We further investigated the effect of acidity on the product distribution in selected RMs. Fig. 6 shows sigmoidal variations in the product distribution on changing the acidity of the solution, at high acidities the major dediazonation products are the substitution ones, and their relative yield depends on the solvent composition; however, at lower acidities, the major dediazonation product is the reduction one, ArH , and its yield is independent of the solvent composition.

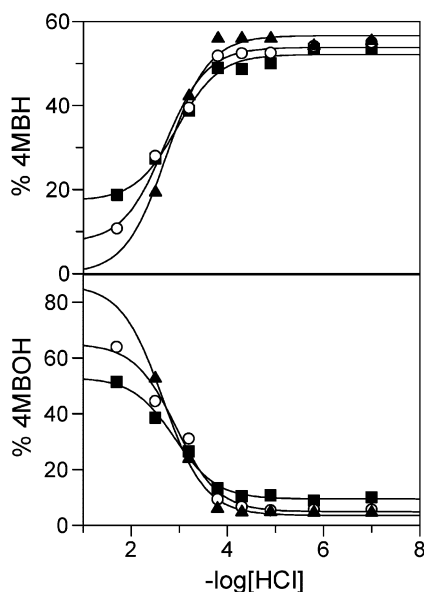
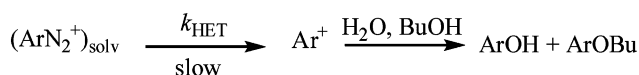


Fig. 6 Effect of the $[\text{HCl}]$ on product distribution for the decomposition of 4MBD in reverse micelle BuOH/SDS/ H_2O . $[\text{4MBD}] \sim 8 \times 10^{-4} \text{ M}$, $T = 50^\circ \text{C}$. ■ 72.5%, ○ 61.9% and ▲ 45% of BuOH.

Discussion

The results of binary mixtures, Table 1, show that k_{obs} increases modestly on increasing %BuOH from 0 up to 98% BuOH. A rate-limiting nucleophilic attack of BuOH would lead to a substantial change in k_{obs} upon changing the BuOH concentration in the reaction mixture, which is not observed. HPLC experiments show that only small amounts of the formation of reduction product ArH are formed. Hence, kinetic and HPLC results are consistent with the well-established $\text{D}_\text{N} + \text{A}_\text{N}$ dediazonation mechanism, *e.g.*, a rate-determining formation a highly reactive aryl cation which traps any available nucleophile in its solvation shell, Scheme 2.



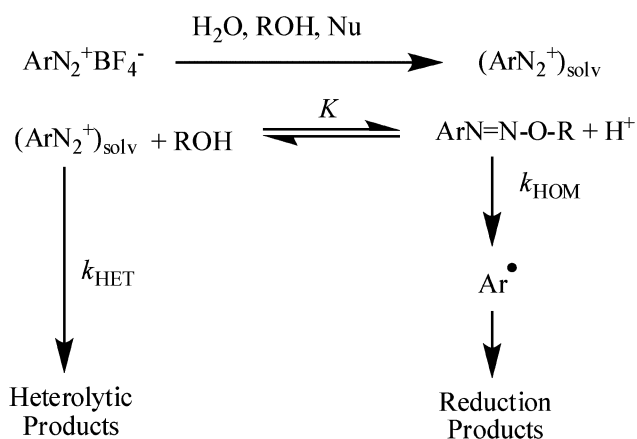
Scheme 2 Basic representation of the $\text{D}_\text{N} + \text{A}_\text{N}$ dediazonation mechanism showing the rate-limiting formation of an extremely reactive aryl cation Ar^+ that traps any available nucleophile in its solvation shell.^{35,39,44,45}

Fig. 1 shows that the sigmoidal variations of k_{obs} with acidity are obtained when employing reaction mixtures with a high BuOH

content, in contrast with the small changes obtained when using reaction mixtures with low BuOH content, Table 2. Fig. 2 displays the S-shaped variation of the product distribution with acidity, showing that at high acidity, low yields of the reduction product ArH are obtained but, on lowering the acidity, ArH becomes the main dediazonation product, suggesting a pH-dependent change in the reaction mechanism. In both cases, the largest variations of k_{obs} and product yields with acidity are found in the $-\log[\text{HCl}] = 2\text{--}5$ range, *i.e.*, under acidic conditions.

S-shaped variations of k_{obs} with acidity are usually observed in reactions of acid–base pairs where both forms are attainable and show different reactivities.⁴⁷ Under our experimental conditions, only two specimens may undergo acid–base processes, the ArN_2^+ ions and BuOH. The $\text{p}K_\text{a}$ of BuOH is ~ 18 and the $\text{p}K_\text{a}$ value of 4MBD has been reported to be ~ 11 ,⁴⁸ so it appears unlikely that ArN_2^+ ions react with BuO^- or with OH^- ions, as in an alkaline medium,^{49,50} under our experimental conditions.

Analogous S-shaped variations of k_{obs} and of the product distribution were observed in previous solvolytic dediazonations and were interpreted in terms of the reaction mechanism shown in Scheme 3, which hypothesizes two competitive reaction pathways, (i) the thermal decomposition of the solvated ArN_2^+ ions through the heterolytic $\text{D}_\text{N} + \text{A}_\text{N}$ mechanism, leading to the formation of substitution products (ArOH , ArOBu) and (ii) the formation of an adduct between ArN_2^+ ions and BuOH in a rapid pre-equilibrium step followed by its rate-determining homolysis, initiating a radical process leading to the formation of the reduction products ArH , Scheme 3. Similar mechanisms have been employed to interpret the reactivity of arenediazonium ions with nucleophilic molecules bearing $-\text{OH}$ groups such as the antioxidants ascorbic acid (vitamin C), gallic acid and methyl gallate, and $-\text{NH}_2$ groups such as the amino acids serine and glycine. The assumption of a rate-limiting decomposition of the diazo ether is also consistent with reported results for other O-coupling reactions,^{35,45,51,52} and was probed experimentally in reactions of arenediazonium ions in the presence of cyclodextrins.^{53,54}



Scheme 3 Proposed competitive ionic and radical mechanisms for the reaction of arenediazonium ions with alcohols under acidic conditions.

From Scheme 3, eqn (1) can be derived where k_{HET} and k_{HOM} are the rate constants for the heterolytic decomposition of ArN_2^+ (Scheme 2) and for the decomposition of the diazo ether which initiates the radical mechanism, respectively, with K standing for

Table 4 Values of the half-lives and activation energies for the heterolytic (HET) and homolytic (HOM) dediazonation processes for some arenediazonium ions in different solvents.

Substituent	Solvent composition	$t_{1/2}$ (HET)/s ^a	$t_{1/2}$ (HOM)/s ^a	E_a (HET)/kJ mol ⁻¹	E_a (HOM)/kJ mol ⁻¹
4-Me	H ₂ O ^b	3450	—	110	—
	70–30 TFE–H ₂ O ^c	1770	—	119	—
	99.5–0.5 MeOH–H ₂ O ^b	1971	—	109	—
	70–30 EtOH–H ₂ O ^d	359	35	116	77
	90–10 BuOH–H ₂ O ^e	1000	144	103	74
	72.5 BuOH ^f	1200	4	—	76
4-NO ₂	H ₂ O ^g	~ 83000	—	119	—
	80–20 MeOH–H ₂ O ^b	15687	1375	—	—
	95–5 MeOH–H ₂ O ^h	3648	1824	—	—
4-Br	H ₂ O ^{g,i}	~ 180000	—	~ 100	—
	25–75 MeOH–H ₂ O ⁱ	—	2390	~ 100	71
	75–25 MeOH–H ₂ O ⁱ	—	2980	~ 100	74

^a $T = 50\text{ }^{\circ}\text{C}$. ^b From ref. 39. ^c From ref. 55. ^d From ref. 63. ^e This work, binary mixture. ^f This work, reverse micelles. ^g From ref. 64. ^h From ref. 46. ⁱ From ref. 55.

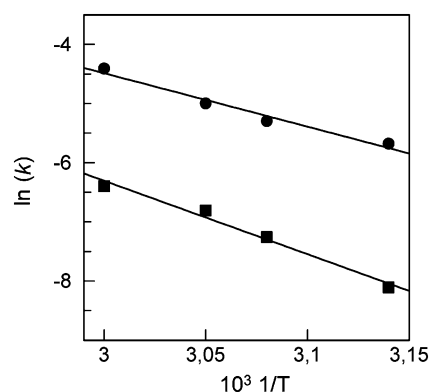
the equilibrium constant of the formation of the diazo ether, Scheme 3.

$$k_{\text{obs}} = \frac{k_{\text{HET}}[\text{H}^+] + k_{\text{HOM}}K[\text{BuOH}]}{K[\text{BuOH}] + [\text{H}^+]} \quad (1)$$

Eqn (1) is typical of processes where an S-shaped dependence of k_{obs} with $-\log[\text{H}^+]$ is observed (where $[\text{H}^+]$ represents the concentration of protonated solvent molecules). From eqn (1), and by considering limits, we find that when $[\text{H}^+] \gg K[\text{BuOH}]$, $k_{\text{obs}} \approx k_{\text{HET}}$, *i.e.*, the reaction proceeds wholly through the D_N + A_N mechanism and only heterolytic products are obtained. On the other hand, when $[\text{H}^+] \ll K[\text{BuOH}]$, $k_{\text{obs}} \approx k_{\text{HOM}}$, *i.e.* the reaction proceeds wholly through the O-diazo ether and formation of reduction products is favored. The solid lines in Fig. 1, 2, 4 and 6 were obtained by fitting the experimental data to eqn (1) by means of a non-linear least-squares method provided by the GraFit 5.0.5 computer program, and the average p*K* value, as well as those for k_{HET} and k_{HOM} , are listed in Table 3.

The variation in equilibrium constant K for the formation of the diazo ether, Table 3, does not show a clear tendency upon changing the temperature, and by considering their average value, the free Gibbs energy for the formation of the diazo ether can be obtained, $\Delta G \approx 30\text{ kJ mol}^{-1}$, indicating that the formation of the diazo ethers is not a spontaneous process. On the other hand, at any temperature $k_{\text{HOM}} \gg k_{\text{HET}}$ in both binary mixtures and reverse micelles, in line with previous reports^{40,46,50,55} but, curiously enough, the k_{HOM} values in the binary mixtures are much lower than those in the reverse micelles. Rate enhancements of the rate of decomposition of diazo ethers (*i.e.*, k_{HOM}) have been previously reported in the presence of normal micelles^{56–58} and thus our results may not be surprising, but the present data can not provide a convincing explanation for this observation because nothing is known about the micellar effects on the reactivity and stability of such adducts in spite of the fact that the bond-rotating mechanism to transform the *Z*-isomer into the much more stable *E*-derivative has been described in aqueous solution.⁵⁹

The activation parameters for the heterolytic and homolytic pathways can be obtained by fitting the k_{HET} and k_{HOM} values in Table 3 to the Arrhenius equation, Fig. 7. The estimated value for the heterolytic process, E_a (HET) = $103 \pm 10\text{ kJ mol}^{-1}$, is in keeping with those reported in the literature.⁶⁰ The activation energy for the

**Fig. 7** Variation of $\ln(k_{\text{HET}})$ (●) and $\ln(k_{\text{HOM}})$ (■) with $1/T$ according to the Arrhenius equation. Data from Table 3.

homolytic process, E_a (HOM) = $75 \pm 9\text{ kJ mol}^{-1}$ (binary mixture) is equal to that obtained in reverse micelles, E_a (HOM) = $77 \pm 6\text{ kJ mol}^{-1}$, and is substantially lower than the activation energy obtained for the heterolytic process. Curiously enough, the E_a (HOM) value for the butanolyses and ethanolyses of 4MBD are the same and are equal to that obtained for the methanolysis of 4-bromobenzenediazonium ions in MeOH–H₂O mixtures, E_a (HOM) = $74 \pm 10\text{ kJ mol}^{-1}$, suggesting that the activation energies for the homolytic breakdown of diazo ethers are not very sensitive to both the nature of the substituents in the aromatic ring and the solvent, Table 4.

It may be instructive to compare the present results with those obtained in other solvolytic dediazoniations. Substituents on the aromatic ring have a marked effect on the stability of arenediazonium ions, and their effects are not understandable in terms of the Hammett equation but can be interpreted in terms of a dual substituent parameter separating the resonance (associated with the ability to transfer charge) and inductive (associated with the polarity) effects. Electron withdrawing substituents such as 4-NO₂ or 4-Br destabilize the aryl cation by induction more than they destabilize the parent arenediazonium ions, and therefore its spontaneous decomposition is much lower than that of the parent, or of arenediazonium ions bearing electron-releasing groups such as 4-Me; compare for instance the half-life value for decomposition of 4MBD in H₂O at $T = 60\text{ }^{\circ}\text{C}$, $t_{1/2} = 3450\text{ s}$,

with that for the decomposition of 4-nitrobenzenediazonium ions at the same temperature, $t_{1/2} \sim 83000$ s (Table 4). However, since arenediazonium ions decompose spontaneously through the formation of an extremely reactive aryl cation ($D_N + A_N$ mechanism, Scheme 2), the k_{HET} values are not very sensitive to changes in solvent composition as shown in this and in previous dediazonation reports.^{35,45,48}

4-Alkyl substituents in the aromatic ring make ArN_2^+ ions less prone to decomposition through homolytic pathways, as opposed to the, for example, 4- NO_2 or 4-Br- derivatives, and the formation of the O-adduct is only detected under relatively basic conditions, and its formation is not dependent on solvent composition and temperature. This observation contrasts with those observed in the methanolyses of 4- NO_2 and 4-Br-arenediazonium ions, where the formation of the diazo ethers depends on both pH and MeOH concentration: at low percentages of ROH, the corresponding diazo ethers are formed because of the equilibrium constant for their formation is high (and consequently the reaction proceeds through the radical mechanism, Scheme 3) but its formation is not so favored at high %ROH in spite of the much higher [ROH] because of the medium effect on K , and in these situations the ionic and radical mechanisms become competitive (Table 4). However, once the diazo ether is formed, it decomposes, initiating a radical process whose activation energy seems to be independent of the nature of the substituent in the aromatic ring (Table 4).

Previous studies on the formation of diazo ethers under alkaline conditions suggest that diazo ethers are initially formed in a highly unstable, kinetically controlled, *Z*-configuration which then may undergo subsequent isomerization to the thermodynamically stable *E*-isomers, which can be isolated in some instances,⁶¹ or eventually may give rise to homolytic rupture of the bonds providing the initiation of a radical process.^{35,40,46,55,58,62,63} This bond rotating mechanism to transform the *Z*- into the *E*-isomer has been described for Sandmeyer hydroxylations and chlorination reactions.⁵⁹

In conclusion, we have been able to investigate the formation and decomposition of transient diazo ethers in the course of the butanolysis of 4MBD by employing binary BuOH/ H_2O mixtures and nanostructured systems such as the reverse micelles, which permit one to overcome the solubility problems of BuOH in water. The reaction also provides an effective method to prepare large amounts of the reduction product ArH under relatively mild conditions, hence providing a simple, effective and practical method for replacing aromatic amino groups by hydrogen, representing an improved alternative to current literature methods.^{35,48,53,65,66}

In reaction mixtures with low BuOH content, a change in the acidity does not change k_{obs} values and only heterolytic dediazonation products are obtained. The results are consistent with the $D_N + A_N$ mechanism, *i.e.*, a rate-limiting formation of an extremely reactive aryl cation that further reacts with available nucleophiles in the solvation shell. However, in reaction mixtures containing a high percentage of BuOH (either BuOH/ H_2O mixtures or BuOH/SDS/ H_2O reverse micelles), S-shaped variations in both k_{obs} and in the product distribution with acidity were observed, with inflection points close to $-\log[\text{HCl}] = 4$. At low acidities, substantial amounts of the reduction product ArH were detected, indicating a change in the reaction mechanism from the heterolytic to the homolytic one. Results can be interpreted in terms of two competitive mechanisms (Scheme 3); the heterolytic $D_N + A_N$

pathway and the competitive radical mechanism comprising the formation of an unstable diazo ether that further decomposes.

Changes in temperature do not seem to have any effect on the product distribution or on the equilibrium constant for the formation of the diazo ether, but do change both the homolytic k_{HOM} and heterolytic k_{HET} rate constants allowing the determination of the corresponding activation parameters and, as expected, the activation energy for the heterolytic mechanism is much higher than that for the homolytic process. The activation energy for the heterolytic process E_a (HET), is very similar to that found in previous reports but that for the homolytic process, E_a (HOM), is much lower and seems to be independent of the nature of the substituents and of the alcohol employed.

Finally, it may be worth noting the utility of reverse micelles to study solvolytic reactions allowing the achievement of alcohol concentrations in the system which otherwise cannot be attained because of solubility or incompatibility problems which are frequently encountered in organic chemistry. To overcome the reagent incompatibility, reverse micelles (and microemulsions) have been proved to be useful as reaction media and their use expands the range of solvents where these reactions can be studied and may open new mechanistic possibilities because of their unique properties.^{27,28,35} In the present case, we have overcome the solubility problem between BuOH and water and were able to study a solvolytic dediazonation reaction whose mechanism can be easily modulated from a heterolytic or ionic mechanism to a homolytic or radical one by just changing the acidity of the solution, allowing the study of the factors that control the turnover of the mechanism of the reaction.

Experimental

Instrumentation

UV-Vis spectra and kinetics experiments were monitored on an Agilent 8453 spectrophotometer equipped with a thermostatted cell carrier attached to a Julabo F12-ED thermostat and a computer for data storage and manipulation. Product analysis was carried out on a WATERS HPLC system equipped with a model 600 quaternary pump, a model 717 automatic injector, a model 2487 dual- λ absorbance detector and a computer for data storage. Products were separated with a Microsorb-MV C-18 (Rainin) reversed-phase column (25 cm length, 4.6 mm internal diameter and 5 μm particle size) with a mobile phase of MeOH- H_2O (50 : 50 v/v), containing 10^{-4} M HCl. The injection volume was 25 μl in all runs and the UV detector was set at 220 and 280 nm.

Reagents and materials

Reagents were of the maximum purity available and used without further purification. 4-Cresol (ArOH), toluene (ArH) and the surfactant sodium dodecyl sulfate (SDS) were purchased from Fluka. BuOH was of HPLC grade from Merck and Acros Organics. Other chemicals were from Riedel de Haen. All solutions were prepared by using Milli-Q grade water. The HCl solutions were prepared by dilution from concentrated commercial HCl and their concentrations were determined by potentiometric measurements.

4-Methylbenzenediazonium, 4MBD, tetrafluoroborate was prepared by employing a non-aqueous procedure as indicated elsewhere⁶⁷ and was purified three times from CH₃CN/cold ether; it was stored in the dark at low temperatures to minimize its decomposition and was recrystallized periodically. The UV-Vis spectrum of 4MBD aqueous in acidic condition show a band centred at $\lambda = 278$ nm. The Beer's law plot (not shown) up to 1.5×10^{-4} M is linear, yielding $\varepsilon_{278} = (146 \pm 1) \times 10^2 \text{ M}^{-1} \text{ cm}^{-1}$ and $\varepsilon_{300} = (59 \pm 1) \times 10^2 \text{ M}^{-1} \text{ cm}^{-1}$, in keeping with published data.⁶⁰

Methods

Kinetic data were obtained from spectrophotometric UV-Vis experiments. In all runs, first order kinetics were found for more than 3 half-lives and the observed rate constants, k_{obs} , were obtained by fitting the variation of the absorbance due to ArN_2^+ loss ($\lambda = 278$ nm) with time to the integrated first-order eqn (2) using a nonlinear least squares method provided by a commercial computer program (GraFit 5.0). Solvolytic reactions were carried out at $T = 50^\circ \text{C}$ except where the effects of temperature were investigated. This temperature was chosen because previous investigations⁶⁰ indicated that convenient rate constants can be achieved.

$$\ln \frac{(A_\infty - A_t)}{(A_\infty - A_0)} = -k_{\text{obs}} t \quad (2)$$

Dediazoniation product distributions were determined at room temperature by analyzing the reaction mixtures once the dediazoniation reaction was finished, *i.e.*, at infinite time. For this purpose, a number of reaction mixtures of the desired composition containing all reagents except 4MBD were prepared in volumetric flasks and thermostated at for about 20 min. Then, aliquots of a freshly prepared 4MBD stock solution (typically 20 μL) were added to the volumetric flasks and left to react for at least 5 h. After the reaction was completed, the solutions were cooled to room temperature and aliquots of these solutions were transferred to HPLC vials and analyzed in triplicate.

Chromatograms showed, in addition to the front peak, three chromatographic peaks. Two of them were unambiguously identified as 4-cresol, ArOH, and toluene, ArH, by means of spiking experiments with authentic samples. The third one was tentatively associated with the substitution product 4-butyl-tolyl-eter, ArOBu, based on our experience in previous solvolytic work and because its peak area increases upon increasing [BuOH]. ArOBu is not a commercial product, it was not synthesized, and its yield was not therefore determined. The absence of this product yield produces a systematic error in the total yields. However, this error does not affect the kinetic results because dediazoniation products are formed competitively (see results). Linear calibration curves (correlation coefficient > 0.999) for converting HPLC peak areas into concentrations were obtained for ArOH and ArH by employing commercial samples dissolved in MeOH. The percentage of a given analyte was determined by means of eqn (3), where $[4\text{MBD}]_0$ stands for the initial concentration of 4MBD, which was estimated by weight as described elsewhere.

$$\text{Yield} = 100 \frac{[\text{Analyte}]}{[4\text{MBD}]_0} \quad (3)$$

Table 5 Composition and some relevant structural parameters of the prepared RMs. ρ_m stands for the macroscopic density of the reverse micellar solution, N stands for the aggregation number, r_{wp} is the radius of the water pool, r_c is the radius of the cell and $r_c - r_{\text{wp}}$ indicates the thickness of the interfacial region where the surfactant and the alcohol are located. Further details on their preparation and how the structural parameters were determined can be found elsewhere.⁷⁰

RM	% H ₂ O	% BuOH	[SDS]/ [BuOH]	ρ_m / g ml ⁻¹	N	$r_{\text{wp}}/\text{\AA}$	$r_c/\text{\AA}$	$r_c - r_{\text{wp}}/\text{\AA}$
1	39.9	45	0.086	0.92	33	23.3	33.4	10.1
2	31.9	56	0.056	0.89	26	21.8	34.4	12.6
3	27.7	61.9	0.043	0.88	24	20.0	33.4	13.4
4	23.4	67.8	0.033	0.86	16	18.6	33.4	14.8
5	20	72.5	0.027	0.85	13	17.3	33.0	15.7
6	14.4	80.1	0.017	0.84	11	15.8	33.8	18.0
7	10.9	84.9	0.013	0.84	9	15.4	36.2	20.8
8	7.4	89.8	0.008	0.83	8	14.7	39.6	24.9

Binary mixtures were prepared by mixing the appropriate amounts of BuOH and water, and molar concentrations were calculated by ignoring the small excess volume of mixed solvents.⁶⁸ Reverse micellar solutions were prepared by employing a fixed $w_o = [\text{H}_2\text{O}]/[\text{SDS}] = 42.7$ ratio according to the phase diagram given by Jobe *et al.*,⁶⁹ allowing variations in the percentage of BuOH from 45% to 90%. RMs were prepared by mixing the appropriate amounts of SDS, H₂O and BuOH (by weight) to get the desired compositions, Table 5, which also shows some relevant, previously determined, structural parameters.^{36,37,41,70} The percentage of BuOH in the reaction mixture is given by volume throughout the text.

References

- P. L. Luisi, B. E. Straub, *Reverse Micelles: Biological and Technological Relevance of Amphiphilic Structures in Apolar Media*, Plenum Press, New York, 1984.
- E. Pramauro and E. Pelizzetti, *TrAC, Trends Anal. Chem.*, 1988, **7**, 260.
- E. Pramauro, E. Pelizzetti, *Surfactants in Analytical Chemistry: Applications of Organized Media*, in *Comprehensive Analytical Chemistry*, Elsevier, NY, 1996.
- G. Behera, B. Mishra, P. Behera and M. Panda, *Adv. Colloid Interface Sci.*, 1999, **82**, 1.
- N. L. Klyachko and A. V. Levashov, *Curr. Opin. Colloid Interface Sci.*, 2003, **8**, 179.
- L. García-Río, J. R. Leis, J. C. Mejuto and M. E. Peña, *Langmuir*, 1994, **10**, 1676–1683.
- N. W. Fadnavis and A. Deshpande, *Curr. Org. Chem.*, 2002, **6**, 393.
- C. M. L. Carvalho and J. M. S. Cabral, *Biochimie*, 2000, **82**, 1063.
- R. Bagwe and C. Kilar, *Langmuir*, 2000, **16**, 905.
- M. P. Pilleni, *Structure and Reactivity in Reverse Micelles*, Elsevier, New York, 1989.
- L. García-Río, J. R. Leis, J. C. Mejuto and M. Perez-Lorenzo, *Pure Appl. Chem.*, 2007, **79**, 1111–1123.
- K. Sawada and M. Ueda, *J. Chem. Technol. Biotechnol.*, 2004, **79**, 369.
- V. Uskokovic and M. Drofenik, *Adv. Colloid Interface Sci.*, 2007, **133**, 23.
- J. J. Silber, E. Abuin and E. Lissi, *Adv. Colloid Interface Sci.*, 1999, **82**, 189.
- C. A. Bunton and G. Savelli, *Adv. Phys. Org. Chem.*, 1987, **22**, 213.
- C. A. Bunton, F. Nome, F. H. Quina and L. S. Romsted, *Acc. Chem. Res.*, 1991, **24**, 357–364.
- G. Savelli, R. Germani, L. Brinch In *Reactions and Synthesis in Surfactants Systems*, ed. J. Texter, Marcell-Dekker, New York, 2001, pp 175–246.
- K. Holmberg, *Eur. J. Org. Chem.*, 2007, 731–742.
- L. García-Río, J. R. Leis and E. Iglesias, *J. Phys. Chem.*, 1995, 12318–12326.

- 20 L. Garcia-Rio, J. R. Leis, J. C. Mejuto and M. Perez-Lorenzo, *Pure Appl. Chem.*, 2007, **79**, 1111–1123.
- 21 G. Astray, A. Cid, L. Garcia Rio, P. Hervella, J. C. Mejuto and M. Pérez-Lorenzo, *Prog. React. Kinet. Mech.*, 2008, **33**, 81–97.
- 22 M. A. Lopez-Quintela, C. Tojo, M. C. Blanco, L. Garcia Rio and J. R. Leis, *Curr. Opin. Colloid Interface Sci.*, 2004, **9**, 264–278.
- 23 D. J. Jobe, H. B. Dunford, M. Pickard, J. F. Holwarth, *Reactions in compartmental liquids*, ed. W. Knoche, Germany, 1989.
- 24 M. A. Lopez-Quintela, C. Tojo, M. C. Blanco, L. García-Rio and J. R. Leis, *Curr. Opin. Colloid Interface Sci.*, 2004, **9**, 264–278.
- 25 M. P. Pileni, J. M. Furois, B. Hickel, *Reactivity Studies in AOT Reverse Micelles*, Plenum Press, London, 1984.
- 26 K. Sawada and M. Ueda, *J. Chem. Technol. Biotechnol.*, 2004, **79**, 369.
- 27 V. Uskokovic and M. Drogenik, *Adv. Colloid Interface Sci.*, 2007, **133**, 23–34.
- 28 M. A. Biasutti, E. Abuin, J. Silber, M. Correa and E. A. Lissi, *Adv. Colloid Interface Sci.*, 2008, **136**, 1–24.
- 29 R. Pazo-Llorente, M. J. Rodriguez-Sarabia, E. Gonzalez-Romero and C. Bravo-Díaz, *Int. J. Chem. Kinet.*, 1999, **31**, 73.
- 30 R. Pazo-Llorente, M. J. Sarabia-Rodriguez, E. Gonzalez-Romero and C. Bravo-Díaz, *Int. J. Chem. Kinet.*, 1999, **31**, 531.
- 31 R. Pazo-Llorente, C. Bravo-Díaz and E. Romero-Gonzalez, *Eur. J. Org. Chem.*, 2003, 3421–3428.
- 32 R. Pazo-Llorente, C. Bravo-Díaz and E. González-Romero, *Eur. J. Org. Chem.*, 2004, 3221–3226.
- 33 R. Pazo-Llorente, H. Maskill, C. Bravo-Díaz and E. González-Romero, *Eur. J. Org. Chem.*, 2006, 2201–2209.
- 34 M. J. Pastoriza-Gallego, C. Bravo-Díaz and E. González-Romero, *Langmuir*, 2005, **21**, 2675.
- 35 H. Zollinger, *Diazo Chemistry I, Aromatic and Heteroaromatic Compounds*, VCH, Weinheim, Germany, 1994.
- 36 E. Rodenas and E. Pérez-Benito, *J. Phys. Chem.*, 1991, **95**, 9496.
- 37 E. Rodenas and E. Pérez-Benito, *J. Phys. Chem.*, 1991, **95**, 4552.
- 38 R. Pazo-Llorente, E. González-Romero and C. Bravo-Díaz, *Int. J. Chem. Kinet.*, 2000, **32**, 210.
- 39 R. Pazo-Llorente, C. Bravo-Díaz and E. González-Romero, *Eur. J. Org. Chem.*, 2003, 3421.
- 40 R. Pazo-Llorente, C. Bravo-Díaz and E. González-Romero, *Eur. J. Org. Chem.*, 2004, 3221.
- 41 M. J. Pastoriza-Gallego, C. Bravo-Díaz and E. González-Romero, *Langmuir*, 2005, **21**, 2675.
- 42 C. Bravo-Díaz, M. Soengas-Fernandez, M. J. Rodriguez-Sarabia and E. Gonzalez-Romero, *Langmuir*, 1998, **14**, 5098.
- 43 M. J. Pastoriza-Gallego and C. Bravo-Díaz, *J. Phys. Org. Chem.*, 2009, **22**, 390–396.
- 44 P. S. J. Canning, K. McCrudden, H. Maskill and B. Sexton, *J. Chem. Soc., Perkin Trans. 2*, 1999, 2735.
- 45 A. F. Hegarty, *Kinetics and Mechanisms of Reactions Involving Diazonium and Diazo Groups*, in *The Chemistry of Diazonium and Diazo Compounds*, ed. S. Patai, J. Wiley & Sons, NY, 1978.
- 46 R. Pazo-Llorente, H. Maskill, C. Bravo-Díaz and E. González-Romero, *Eur. J. Org. Chem.*, 2006, 2201.
- 47 R. G. Wilkins, *Kinetics and Mechanism of Reactions of Transition Metal Complexes*, VCH-New York, 1991.
- 48 K. H. Saunders, R. L. M. Allen, *Aromatic Diazo Compounds*, Edward Arnold, Baltimore, MD, 3rd edn, 1985.
- 49 T. J. Broxton, J. F. Bunnett and C. H. Paik, *J. Org. Chem.*, 1977, **42**, 643–649.
- 50 J. F. Bunnett and C. Yijima, *J. Org. Chem.*, 1977, **42**, 639–643.
- 51 W. J. Boyle, T. Broxton and J. F. Bunnett, *J. Chem. Soc. Chem. Commun.*, 1971, **22**, 1469.
- 52 J. F. Bunnett and H. Takayama, *J. Org. Chem.*, 1968, **33**, 1924.
- 53 E. González-Romero, B. Malvido-Hermelo and C. Bravo-Díaz, *Langmuir*, 2002, **18**, 46.
- 54 E. González-Romero, B. Fernández-Calvar and C. Bravo-Díaz, *Prog. Colloid Polym. Sci.*, 2004, **123**, 131.
- 55 A. Fernández-Alonso and C. Bravo-Díaz, *Org. Biomol. Chem.*, 2008, **6**.
- 56 U. Costas Costas, C. Bravo-Díaz and E. González-Romero, *Langmuir*, 2005, **21**, 10983–10991.
- 57 U. Costas-Costas, C. Bravo-Díaz and E. González-Romero, *Langmuir*, 2003, **19**, 5197–5203.
- 58 U. Costas-Costas, C. Bravo-Díaz and E. González-Romero, *Langmuir*, 2004, **20**, 1631–1638.
- 59 P. Hanson, J. R. Jones, A. B. Taylor, P. H. Walton and A. W. Timms, *J. Chem. Soc., Perkin Trans. 2*, 2002, 1135.
- 60 M. C. Garcia-Meijide, C. Bravo-Díaz and L. S. Romsted, *Int. J. Chem. Kinet.*, 1998, **30**, 31–39.
- 61 M. P. Doyle, C. L. Nesloney, M. S. Shanklin, C. A. Marsh and K. C. Brown, *J. Org. Chem.*, 1989, **54**, 3785.
- 62 U. Costas-Costas, E. Gonzalez-Romero and C. Bravo Díaz, *Helv. Chim. Acta*, 2001, **84**, 632–648.
- 63 A. Fernández-Alonso and C. Bravo-Díaz, *Helv. Chim. Acta*, 2010, **93**, 877.
- 64 M. L. Crossley, R. H. Kienle and C. H. Benbrook, *J. Am. Chem. Soc.*, 1940, **62**, 1400–1404.
- 65 N. A. Kornblum, G. D. Cooper and J. E. Taylor, *J. Am. Chem. Soc.*, 1950, **72**, 3013.
- 66 C. Bravo-Díaz, M. E. Romero-Nieto and E. Gonzalez-Romero, *Langmuir*, 2000, **16**, 42–48.
- 67 C. Bravo-Díaz and E. González-Romero, *J. Chromatogr., A*, 2003, **989**, 221–229.
- 68 H. Yamamoto, K. Ichikawa and J. Tokunaga, *J. Chem. Eng. Data*, 1994, **39**, 155.
- 69 D. J. Jobe, H. B. Dunford, M. Pickard, J. F. Holwarth, *Reactions in Compartmental Liquids*, ed. W. Knoche, Springer Verlag, Heidelberg, Germany, 1989.
- 70 M. J. Pastoriza-Gallego, C. Bravo-Díaz and E. González-Romero, *Colloids Surf., A*, 2004, **249**, 25.